On the Stability of the Discrete Generalized Multigroup Method

Nathan A. Gibson, Benoit Forget

Department of Nuclear Science and Engineering
Massachusetts Institute of Technology
77 Massachusetts Avenue, Rm. NW12-311
Cambridge, MA 02139

Abstract

This paper investigates the stability of the recondensation procedure of the Discrete Generalized Multigroup method and proposes alternatives to improve stability of the original formulation. Instabilities are shown to happen when employing a simple Picard fixed point iteration and an ill-informed group mapping scheme. This work presents a mapping procedure that improves stability of the original method for fine group calculations. Additionally, a relaxation scheme, Krasnoselskij iteration, is introduced to the fixed point iteration to further improve the stability characteristics and remove the need for fine group flux updates. Both improvements are applied on heterogeneous problems using the SHEM361 and the NG2042 group structures. The results indicate improve stability from a well-informed group mapping and demonstrate the possibility of eliminating the need for fine group flux updates.

1. Introduction

Deterministic reactor physics methods are currently the industry standard for neutronics modeling and design of nuclear reactors. Deterministic calculations fall into the multigroup energy discretization framework, and their accuracy is entirely dependent upon accurate multigroup cross section data.

For today's light water reactors, cores are modeled with sufficient accuracy using a multi-level approach, where several levels of calculations are used to correctly process multigroup cross sections. First, simplistic geometries are modeled with detailed energy dependence; next, several levels of increasing spatial complexity and decreasing energy resolution are performed. The process of moving from a finer energy structure to a coarser energy structure is known as energy condensation. The success of this process is dependent upon energy spectrum effects being localized.

At the first level, evaluated nuclear data is processed into group cross sections. This is done using the NJOY nuclear data processing system [1]. From evaluated nuclear data files, resonances are reconstructed to produce a point-wise cross section.

Next, a self-shielding step is performed. In some cases, this step is performed with NJOY's `groupr` module, using an assumed flux shape. Fine group cross sections ($\mathcal{O}(50-400)$ groups) are then generated

as a function of background. Alternatively, hyper-fine group cross sections ($\mathcal{O}(1000-10000)$ groups) can be generated and used in a very simple spatial calculation, usually a pin-cell or an infinite medium. This calculation is used to produce the fine group cross section set.

At the next level, lattice calculations are performed with $\mathcal{O}(50-400)$ groups. The spatial complexity is increased to model a single assembly in the reactor with reflective boundary conditions. These calculations are generally performed with transport theory with detailed spatial and angular representation, using the method of characteristics, the collision probability method, or the discrete ordinates method. Lattice calculations are used to generate a reactor database, including broad-group cross sections ($\mathcal{O}(2-20)$ groups) as a function of temperature and burn-up.

Finally, the full core calculation is performed. This increases the spatial scale to that of the full reactor, but the angular and spatial detail is decreased to homogenized regions. The industry standard for these calculations is nodal diffusion theory.

Although this approach has been very successful in the modeling of classical light water reactors (LWRs), each energy condensation step introduces errors arising from the approximations involved. As novel reactor types are suggested and complexities are added to existing reactors, the cross section energy condensation process is showing its limitations. For instance, the reflective boundary conditions used at the lattice level assume that there is not much interaction between lattices. While this is a somewhat reasonable assumption in current LWRs, this assumption breaks down as different reactor design ideas are considered. For instance, fast reactors and graphite moderated reactors have much longer mean free paths, causing neighboring effects to be more pronounced. These issues can even be seen in more familiar reactor types. For instance, they are seen in LWRs with MOX assemblies neighboring UO_2 assemblies.

1.1. Recondensation

In order to move to higher fidelity and more flexible solution methodologies, the multi-level framework must either be modified or avoided. Although full core continuous energy Monte Carlo simulations are now possible [2, 3], these are not yet suitable for use in design and operational calculations. Similarly, full core deterministic transport calculations are being considered. These, too, are not suitable for design and operational calculations, and they still require cross sections from a similar multi-level approach.

Recent work has sought to retain computational efficiency by modifying rather than avoiding the multi-level framework. By introducing a feedback loop into the procedure, cross sections can be improved. For instance, if information from the full core solution can be used to influence the cross sections used for the full core solution through an iterative process, the solution can be significantly improved. This idea is seen in the Discrete Generalized Multigroup method [4], in similar work with the Consistent Generalized Energy Condensation method [5], and in a somewhat different form in the Embedded Self-Shielding Method [6].

2. Methods Description

2.1. Discrete Generalized Multigroup Method

The improved recondensation procedure presented here uses the Discrete Generalized Multigroup (DGM) method. This framework was first introduced in [7, 8] and has been further developed in [4, 9, 10]. For completeness, this method is presented here. Notation used in this paper has been changed compared to previous publications in order to improve clarity.

First, consider the multigroup transport equation:

$$\begin{aligned}\hat{\Omega}\cdot\psi_g(\vec{r},\hat{\Omega})+\Sigma_{t,g}(\vec{r})\psi_g(\vec{r},\hat{\Omega})\\ =\frac{1}{4\pi}\sum_{g'=1}^{N_g}\Sigma_{s,g'\to g}(\vec{r})\phi_{g'}(\vec{r})+\frac{\chi_g}{4\pi k}\sum_{g'=1}^{N_g}\nu\Sigma_{f,g'}(\vec{r})\phi_{g'}(\vec{r}).\end{aligned}\tag{1}$$

Isotropic scattering is assumed for simplicity but is not a requirement of this derivation. Likewise, the k-eigenvalue formulation is presented, but can easily be extended to time dependent problems. The fine group total cross section is assumed not to be a function of $\hat{\Omega}$.

Next, the energy groups are divided into coarse groups. Each fine group g is assumed to be contained inside some coarse group G:

$$\begin{aligned}\hat{\Omega}\cdot\psi_g(\vec{r},\hat{\Omega})+\Sigma_{t,g}(\vec{r})\psi_g(\vec{r},\hat{\Omega})\\ =\frac{1}{4\pi}\sum_{G'=1}^{N_G}\sum_{g'\in G'}\Sigma_{s,g'\to g}(\vec{r})\phi_{g'}(\vec{r})+\frac{\chi_g}{4\pi k}\sum_{G'=1}^{N_G}\sum_{g'\in G'}\nu\Sigma_{f,g'}(\vec{r})\phi_{g'}(\vec{r}).\end{aligned}\tag{2}$$

Discrete basis functions $\hat{\xi}_i^G$ are introduced. In this notation, the argument of the basis function is assumed to be shifted such that the fine group index can be used directly. The superscript G indicates the coarse group and thus also implies the number of fine groups in that coarse group. The discrete basis functions can be any number of basis sets. Because this derivation assumes unity weights and orthogonal bases, Discrete Legendre Polynomials or Discrete Cosine Transforms (Type II) are implied. However, Discrete Tchebyshev Polynomials, Discrete Wavelet Transforms, or various other basis choices can be used with only minor alterations to the derivation.

Each term is multiplied by the discrete basis function and summed over the fine groups in the coarse group:

$$\begin{aligned}\hat{\Omega}\cdot\sum_{g\in G}\hat{\xi}_i^G(g)\psi_g(\vec{r},\hat{\Omega})+\sum_{g\in G}\hat{\xi}_i^G(g)\Sigma_{t,g}(\vec{r})\psi_g(\vec{r},\hat{\Omega})\\ =\sum_{g\in G}\hat{\xi}_i^G(g)\frac{1}{4\pi}\sum_{G'=1}^{N_G}\sum_{g'\in G'}\Sigma_{s,g'\to g}(\vec{r})\phi_{g'}(\vec{r})\\ +\sum_{g\in G}\hat{\xi}_i^G(g)\frac{\chi_g}{4\pi k}\sum_{G'=1}^{N_G}\sum_{g'\in G'}\nu\Sigma_{f,g'}(\vec{r})\phi_{g'}(\vec{r}).\end{aligned}\tag{3}$$

Flux moments are then defined as:

$$\psi_{i,G}(\vec{r},\hat{\Omega}) = \sum_{g\in G} \hat{\xi}_i^G(g)\psi_g(\vec{r},\hat{\Omega}) \tag{4}$$

$$\phi_{i,G}(\vec{r}) = \sum_{g\in G} \hat{\xi}_i^G(g)\phi_g(\vec{r}). \tag{5}$$

DGM cross sections are defined as:

$$\Sigma_{t,0,G}(\vec{r}) = \frac{\sum_{g\in G} \hat{\xi}_0^G(g)\Sigma_{t,g}(\vec{r})\phi_g(\vec{r})}{\sum_{g\in G} \hat{\xi}_0^G(g)\phi_g(\vec{r})} = \frac{\sum_{g\in G} \Sigma_{t,g}(\vec{r})\phi_g(\vec{r})}{\sum_{g\in G} \phi_g(\vec{r})} \tag{6}$$

$$\delta_{i,G}(\vec{r},\hat{\Omega}) = \frac{\sum_{g\in G} \hat{\xi}_i^G(g)\left(\Sigma_{t,g}(\vec{r}) - \Sigma_{t,0,g}(\vec{r})\right)\psi_g(\vec{r},\hat{\Omega})}{\sum_{g\in G} \psi_g(\vec{r},\hat{\Omega})} \tag{7}$$

$$\Sigma_{s,i,G'\to G}(\vec{r}) = \frac{\sum_{g\in G} \hat{\xi}_i^G(g)\sum_{g'\in G'} \Sigma_{s,g'\to g}(\vec{r})\phi_{g'}(\vec{r})}{\sum_{g'\in G'} \phi_{g'}(\vec{r})} \tag{8}$$

$$\nu\Sigma_{f,G}(\vec{r}) = \frac{\sum_{g\in G} \hat{\xi}_i^G(g)\nu\Sigma_{f,g}(\vec{r})\phi_g(\vec{r})}{\sum_{g\in G} \phi_g(\vec{r})} \tag{9}$$

$$\chi_{i,G} = \sum_{g\in G} \hat{\xi}_i^G(g)\chi_g. \tag{10}$$

In the definition of the DGM cross sections, the total cross section is split into two terms, $\Sigma_{t,0,G}$ and $\delta_{i,G}$. $\Sigma_{t,0,g}$ is defined so as not to depend on $\hat{\Omega}$, and $\delta_{i,G}$ is a correction term to retain the angular dependence. This formulation enhances stability, as it avoids putting higher order flux moments—which may be arbitrarily small—in the denominator.

The DGM equations are then:

$$\begin{aligned}\hat{\Omega}\cdot\psi_{i,G}(\vec{r},\hat{\Omega}) + \Sigma_{t,0,G}(\vec{r})\psi_{i,G}(\vec{r},\hat{\Omega}) + \delta_{i,G}(\vec{r},\hat{\Omega})\psi_{0,G}(\vec{r},\hat{\Omega}) \\ = \frac{1}{4\pi}\sum_{G'=1}^{N_G} \Sigma_{s,i,G'\to G}(\vec{r})\phi_{0,G'}(\vec{r}) + \frac{\chi_{i,g}}{4\pi k}\sum_{G'=1}^{N_G} \nu\Sigma_{f,G'}(\vec{r})\phi_{0,G'}(\vec{r}).\end{aligned} \tag{11}$$

The zeroth order, or $i = 0$, DGM equation is entirely equivalent to a coarse group multigroup problem with cross sections collapsed by the standard procedure. The higher order, $i > 0$, equations are purely absorbing fixed source equations, the solution to which give shape information regarding the fine group flux. Because the right hand side of the higher order equations do not depend upon their own solutions, they are not eigenproblems. This is most easily seen by recasting the equations in operator notation:

$$\begin{aligned}\mathbb{T}_0\Psi_0 &= \mathbb{S}_0\Phi_0 + \frac{1}{k}\mathbb{F}_0\Phi_0 \qquad i = 0 \\ \mathbb{T}_i\Psi_i &= \mathbb{S}_i\Phi_0 + \frac{1}{k}\mathbb{F}_i\Phi_0 \qquad i > 0,\end{aligned} \tag{12}$$

where $\mathbb{T}$ is the streaming and collision transport operator, $\mathbb{S}$ is the scattering matrix, $\mathbb{F}$ is the fission matrix, Ψ and Φ are the angular and scalar flux vectors, and the subscripts are the energy moments.

After solving these equations, the fine group flux can be unfolded from the flux moments:

$$\psi_g(\vec{r},\hat{\Omega}) = \sum_{i=0}^{N_G-1} a_i \hat{\xi}_i^G(g)\psi_{i,G}(\vec{r},\hat{\Omega}) \tag{13}$$

$$\phi_g(\vec{r}) = \sum_{i=0}^{N_G-1} a_i \hat{\xi}_i^G(g)\phi_{i,G}(\vec{r}), \tag{14}$$

where a_i is a property of the chosen discrete basis set.

This unfolded flux is an approximation of the fine group flux. However, it is limited in accuracy by the choice of the guessed flux used to weight the DGM cross sections from Eqs. 6–10.

Recognizing that the unfolded flux is a better approximation to the true solution than the initial guessed flux, an intuitive procedure is to add an iteration step to the DGM procedure. Because cross sections are initially condensed with a guessed flux and subsequently condensed again with an improved flux, this iteration procedure is called *recondensation*.

When a flat in-mesh flux approximation is used, the DGM equations are fully consistent with the fine group transport problem. Thus, the recondensation procedure will converge to the true fine group flux [4]. However, this procedure was introduced not to fully compute the fine group flux but rather to improve condensed cross sections with a relatively few number of iteration steps. If a higher order in-mesh flux approximation is used (*e.g.* diamond difference, step characteristics), spatial inconsistencies arise, but significant accuracy can still be obtained [11].

In the multi-level approach of Sec. 1, this allows information from one level to be fed back to the previous level to improve the coarsened cross sections. For instance, if DGM is used on a core level calculation and unfolds the flux to the energy structure of the lattice calculation, corrections to account for reflective boundary conditions improperly representing neighboring effects can be captured. If used on a lattice level calculation, unfolding to the energy structure of the self-shielding level, spatial self-shielding effects not previously captured can be picked up.

In previous work by Zhu [4], the recondensation procedure was not found to be stable in general. This was addressed by adding a flux update step after the unfolding. A flux update is a single purely absorbing fine group sweep using a fixed source built from the unfolded spectrum:

$$\hat{\Omega}\cdot\nabla\psi_g^{\text{update}} + \Sigma_{t,g}\psi_g^{\text{update}} = \frac{1}{4\pi}\sum_{G'=1}^{N_G}\sum_{g'\in G'}\Sigma_{s,g'\to g}\phi_{g'} + \frac{\chi_g}{4\pi k}\sum_{G'=1}^{N_G}\sum_{g'\in G'}\nu\Sigma_{f,g'}\phi_{g'}. \tag{15}$$

Initial work to address stability concerns was presented in [12]. This work is expanded and explored more deeply in this paper.

2.2. Fixed Point Iteration

The recondensation procedure discussed previously is an example of fixed point iteration. Details regarding this class of problems are presented here.

Fixed point iteration is the process of solving the equation $x = \mathbb{A}x$, where x is a vector and $\mathbb{A}$ is some operator that can act on x. A given operator may have a unique fixed point, no fixed points, or multiple fixed points.

2.2.1. Picard Iteration

The most intuitive solution technique is Picard iteration or the sequence of successive approximations [13]. The scheme starts with a guessed solution vector $x^{(0)}$, and subsequent iterates $x^{(n)}$ are obtained by applying the operator:

$$x^{(n+1)} = \mathbb{A}x^{(n)}. \tag{16}$$

In practice, a solution is obtained when the difference between successive iterates, under some norm $||\cdot||$, is within a tolerance ϵ:

$$||x^{(n+1)} - x^{(n)}|| < \epsilon. \tag{17}$$

This procedure, however, is not guaranteed to converge in general. Rather, it requires that the operator $\mathbb{A}$ be contractive. For any two vectors y_1 and y_2, that is:

$$||\mathbb{A}y_1 - \mathbb{A}y_2|| < ||y_1 - y_2||. \tag{18}$$

This is equivalent to requiring the distance between successive Picard iterates decreases. Also, because at the solution x^*, the equality $\mathbb{A}x^* = x^*$ holds true, this implies that each successive iterate more closely approximates the solution than the previous:

$$||x^* - \mathbb{A}x^{(n)}|| < ||x^* - x^{(n)}||. \tag{19}$$

An operator in which Picard iteration is convergent can be categorized as a θ-contraction:

$$||\mathbb{A}y_1 - \mathbb{A}y_2|| \leq \theta||y_1 - y_2|| \qquad \theta \in [0, 1). \tag{20}$$

The value of θ can be used to determine a bound on the convergence rate of Picard iteration, with smaller values of θ leading to faster convergence.

2.2.2. Krasnoselskij Iteration

If an operator does not satisfy the contractive condition in Eq. 18, another iteration scheme is needed to solve the fixed point problem. The Krasnoselskij iteration [14, 13] is one such iteration procedure. With $\lambda \in (0, 1]$ as a fixed parameter, it is given by:

$$x^{(n+1)} = (1 - \lambda)x^{(n)} + \lambda\mathbb{A}x^{(n)}. \tag{21}$$

In the case of $\lambda = 1$, this reduces exactly to Picard iteration. More generally, Krasnoselskij is equivalent to Picard iteration where the operator is taken to be $\mathbb{A}_\lambda = (1 - \lambda)\mathbb{I} + \lambda\mathbb{A}$, with $\mathbb{I}$ being the identity operator. This modified operator $\mathbb{A}_\lambda$ requires a weaker condition on the operator $\mathbb{A}$ for convergence of the iteration: that it be Lipschitzian [13]. That is, there exists a finite $L > 0$ such that:

$$||\mathbb{A}y_1 - \mathbb{A}y_2|| < L||y_1 - y_2||. \tag{22}$$

In practice, the value of λ is a degree of freedom in an implementation of Krasnoselskij iteration. For a given operator, there exists some λ_{max} above which the iteration procedure will not be stable. In general, λ_{max} need not be the optimal choice of λ for the fastest convergence. In fact, in some cases where Picard iteration converges, Krasnoselskij iteration with $\lambda < 1$ may converge faster.

Thus, there is also an optimal value λ_{opt} for which Krasnoselskij iteration converges the fastest. One must define the meaning of optimal in this context. In mathematics literature, λ_{opt} is obtained by minimizing the effective θ from Eq. 20 [13]. However, this provides the optimal bound on the convergence rate but not necessarily the optimal convergence rate. For this study λ_{opt} will be considered the value of λ for which a solution within a given tolerance is achieved in the fewest iterations. Note that by this definition, λ_{opt} may be a function of not only the operator $\mathbb{A}$ but also the starting guess $x^{(0)}$.

2.2.3. Mann Iteration

Another fixed point iteration scheme is Mann iteration [13], a straightforward extension of Krasnoselskij. In Mann, λ is replaced with $a^{(n)} \in (0, 1]$ which is allowed to vary by iteration:

$$x^{(n+1)} = \left(1 - a^{(n)}\right) x^{(n)} + a^{(n)}\mathbb{A}x^{(n)}. \tag{23}$$

For many problems, stability issues are magnified near the fixed point. Mann iteration allows larger steps to be taken when far from the fixed point and smaller steps near the solution to preserve stability.

Of course, many other iteration schemes exist, but these are not presented here.

2.3. Cross Section Group Structures

Two cross section group structures are used in this study, the SHEM361 and NG2042 structures.

The SHEM361 structure [15, 16] was introduced to reduce the need for self-shielding calculation for low-lying resonances. The most common and significant isotopes encountered in reactor simulations, including actinides, fission products, absorbers, moderators/coolants, and structural materials were considered. The whole of these isotopes' resonance structure was considered up to 11.4 keV. Above this range, significant effects such as threshold reactions and other large resonances in U-238 were considered. The mesh sought to account for issues such as the mutual self-shielding effects of overlapping low-lying resonances.

The NG2042 structure is introduced by the author as a compromise between using a true ultrafine library and using a tractable number of groups in calculations. A mesh like SHEM361 does not behave as an ultrafine library, as resonances are not fully resolved. A true ultrafine library introduces significant complications, including long run times and large memory requirements. The NG2042 structure makes no attempt to optimize group selection and is certainly inadequate to resolve resonances. However, it has enough groups that libraries using it behave much like ultrafine libraries while having a more reasonable runtime. In the thermal region, NG2042 uses the TRESFIN 524-group energy block used in CEA's 11,276-group structure [17]. Above thermal energies, groups are given equal lethargy widths of $\Delta u = 1/100$. The result is a 2042-group energy mesh.

3. Simplest Example of Stability Issues

3.1. Description

In order to study the stability of the DGM procedure, consider the simplest possible DGM problem: two fine groups mapped to a single coarse group in an infinite medium. For simplicity, there is no up-scattering and all fission neutrons are born in the fast group. For this problem, the fine group equations are:

$$\begin{aligned} \Sigma_{t,1}\phi_1 &= \Sigma_{s,1\to1}\phi_1 + \frac{1}{k}\left(\nu\Sigma_{f,1}\phi_1 + \nu\Sigma_{f,2}\phi_2\right) \\ \Sigma_{t,2}\phi_2 &= \Sigma_{s,1\to2}\phi_1 + \Sigma_{s,2\to2}\phi_2. \end{aligned} \tag{24}$$

The discrete basis set is chosen to be Discrete Legendre Orthogonal Polynomials:

$$\begin{aligned} \xi_0 &= \begin{bmatrix} 1 & 1 \end{bmatrix} \\ \xi_1 &= \begin{bmatrix} 1 & -1 \end{bmatrix}. \end{aligned} \tag{25}$$

The flux moments are then:

$$\begin{aligned} \varphi_0 &= \phi_1 + \phi_2 \\ \varphi_1 &= \phi_1 - \phi_2, \end{aligned} \tag{26}$$

and the unfolded flux is:

$$\begin{aligned}\phi_1 &= \frac{1}{2}\left(\varphi_0 + \varphi_1\right) \\ \phi_2 &= \frac{1}{2}\left(\varphi_0 - \varphi_1\right).\end{aligned} \tag{27}$$

The DGM equations are thus:

$$\begin{aligned}\Sigma_{t,0,G}\varphi_0 &= \Sigma_{s,0,G}\varphi_0 + \frac{1}{k}\nu\Sigma_{f,G}\varphi_0 \\ \Sigma_{t,0,G}\varphi_1 + \delta_{1,G}\varphi_0 &= \Sigma_{s,1,G}\varphi_0 + \frac{1}{k}\nu\Sigma_{f,G}\varphi_0,\end{aligned} \tag{28}$$

where the DGM cross sections are given by:

$$\Sigma_{t,0,G} = \frac{\Sigma_{t,1}\phi_1 + \Sigma_{t,2}\phi_2}{\phi_1 + \phi_2} \tag{29}$$

$$\delta_{1,G} = \frac{\left(\Sigma_{t,1} - \Sigma_{t,0,g}\right)\phi_1 - \left(\Sigma_{t,2} - \Sigma_{t,0,g}\right)\phi_2}{\phi_1 + \phi_2} \tag{30}$$

$$\Sigma_{s,0,G} = \frac{\left(\Sigma_{s,1\to1} + \Sigma_{s,1\to2}\right)\phi_1 + \Sigma_{s,2\to2}\phi_2}{\phi_1 + \phi_2} \tag{31}$$

$$\Sigma_{s,1,G} = \frac{\left(\Sigma_{s,1\to1} + \Sigma_{s,1\to2}\right)\phi_1 - \Sigma_{s,2\to2}\phi_2}{\phi_1 + \phi_2} \tag{32}$$

$$\nu\Sigma_{f,G} = \frac{\nu\Sigma_{f,1}\phi_1 + \nu\Sigma_{f,2}\phi_2}{\phi_1 + \phi_2}. \tag{33}$$

Because this is an eigenproblem, the solution $\begin{bmatrix}\phi_1 & \phi_2\end{bmatrix}^T$ has a multiplicative degree of freedom. Thus, it can be fully defined with the thermal-to-fast flux ratio $f = {}^{\phi_2}/_{\phi_1}$.

The standard solution methodology is to cast the DGM problem as a fixed-point iteration. The DGM equations take guesses of ϕ_1 and ϕ_2—or equivalently f—as an input to collapse the cross sections with Eqs. 29–33. They are then solved to produce updated values, $\tilde{\phi}_1$ and $\tilde{\phi}_2$ or $\tilde{f}$. The DGM operator is notated as $\mathbb{D}$. The updated values can be used to define the input for the next iteration. The solution is achieved when $f = \tilde{f}$ within some tolerance.

The most intuitive fixed point iteration scheme is Picard iteration, described in Sec. 2.2.1:

$$f^{(n+1)} = \mathbb{D}(f^{(n)}) \equiv \tilde{f}^{(n)}. \tag{34}$$

3.2. Numerical Examples

Now, consider a numerical example with this simple problem. Take the fine group cross sections to be:

$$\begin{aligned} \Sigma_{t,1} &= 1 \text{ cm}^{-1} \quad \Sigma_{t,2} = 2 \text{ cm}^{-1} \\ \Sigma_{s,1\to1} &= \Sigma_{s,1\to2} = \Sigma_{s,2\to2} = 0.3 \text{ cm}^{-1} \\ \nu\Sigma_{f,1} &= \nu\Sigma_{f,2} = 0.5 \text{ cm}^{-1}. \end{aligned} \tag{35}$$

Using $f_0 = 1$ as the starting seed for Picard iteration, the true solution of $f = 0.1765$ and $k = 0.8403$ is obtained within 10^{-5} on eigenvalue in 39 iterations.

Next, consider a second problem in which the same cross sections are used, changing only the value of $\Sigma_{t,2}$:

$$\Sigma_{t,2} = 3 \text{ cm}^{-1}. \tag{36}$$

Again using $f_0 = 1$ as the starting seed for Picard iteration, the true solution of $f = 0.1111$ and $k = 0.7937$ is not obtained. Rather than approaching this solution, the iterates quickly diverge. Negative fluxes are seen after only a single iteration.

To understand this behavior, consider the stability requirements of Picard iteration, as presented in Sec. 2.2.1. The requirement that the operator be contractive is equivalent to requiring the spectral radius of the operator be less than unity. For a univariate fixed point scheme such as this one, the spectral radius ρ is the magnitude of the derivative of the output y with respect to the input x:

$$\rho = \left| \frac{dy}{dx} \right|. \tag{37}$$

By evaluating the DGM operator over a full range of input f values, a plot of input versus output and the derivative can be generated. Figure 1 shows this plot for the first case, with $\Sigma_{t,2} = 2 \text{ cm}^{-1}$; Fig. 2 shows this plot for the second case, with $\Sigma_{t,2} = 3 \text{ cm}^{-1}$.

In these plots, the solution is the intersection of $f(x)$ and the line $y = x$. At the solution, for the first case, the magnitude of the derivative is seen to be less than unity; thus, a Picard iteration procedure starting in a neighborhood about the solution is expected to converge to the solution.

For the second case, the magnitude of the derivative is seen to be greater than unity at the solution; thus, the scheme is unstable, and Picard iteration is not expected to converge to the solution from any starting guess.

Even in this extremely simple example, stability issues pertaining to the DGM recondensation procedure can be seen. For any physical problem, without modification, the DGM procedure cannot be expected to be stable in general. The following section will explore means of improving the stability characteristics.

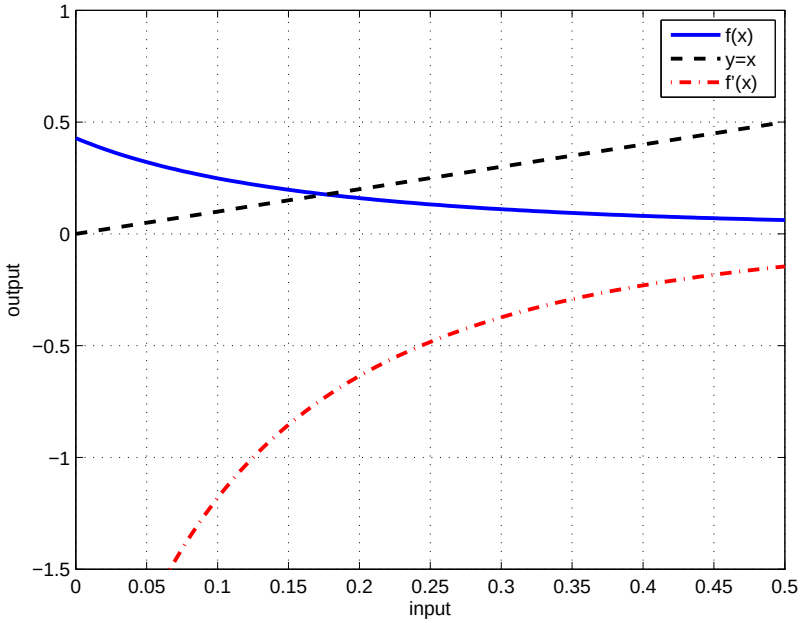

Figure 1: Input versus output thermal to fast flux ratios for stable DGM case

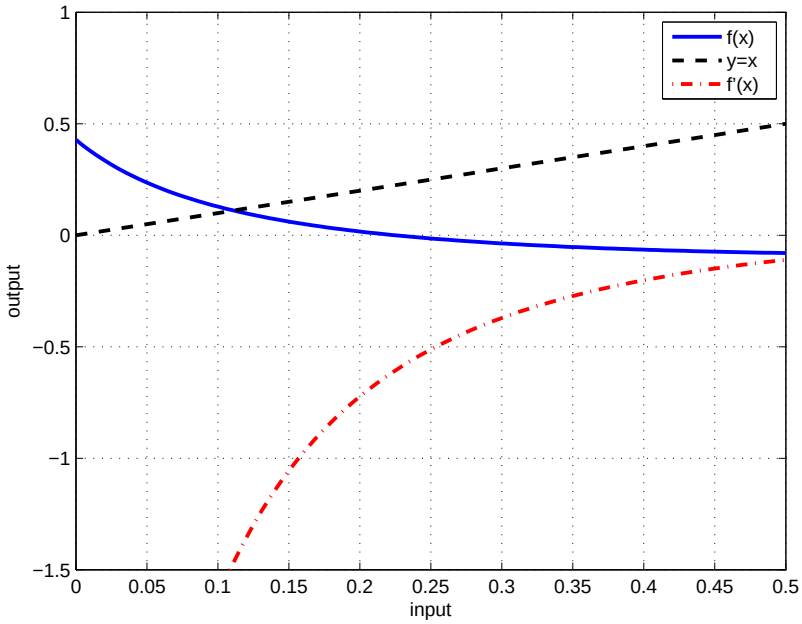

Figure 2: Input versus output thermal to fast flux ratios for unstable DGM case

4. Improving Stability of Iteration Scheme

4.1. Flux Updates

In past work [4], stability concerns were addressed through the use of flux updates, previously shown as Eq. 15. These flux updates add a fine group fixed source sweep to the operator, making Picard iteration stable. The unfolded flux from the solution of the DGM equations is used to build a fixed scattering and fission source, and a transport sweep is performed to obtain a new flux. For the simple problem presented in Sec. 3.1, the flux update is simply:

$$\begin{aligned} \phi_1^{\text{update}} &= \frac{\Sigma_{s,1\to1}\phi_1 + \frac{1}{k}\left(\nu\Sigma_{f,1}\phi_1 + \nu\Sigma_{f,2}\phi_2\right)}{\Sigma_{t,1}} \\ \phi_2^{\text{update}} &= \frac{\Sigma_{s,1\to2}\phi_1 + \Sigma_{s,2\to2}\phi_2}{\Sigma_{t,2}}. \end{aligned} \tag{38}$$

When a flux update is added to the DGM operator in the simple example, the previously unstable case, with $\Sigma_{t,2} = 3$ cm^{-1}, stably converges to the true solution. The flux update essentially provides the convergence properties of the fine group problem. Figure 3 shows the input versus output and derivative plot. The magnitude of the derivative at the solution is less than unity, and so the procedure is expected to be convergent, as is observed in practice.

If DGM is thought of as a multigrid procedure in energy, flux updates are essentially the smoother applied at the fine grid. However, as increasingly difficult problems are encountered, several consecutive flux updates may be needed to obtain stability. Also, for these difficult problems, flux updates become increasingly expensive and can represent a large fraction of the overall computational time associated with the method.

4.2. Krasnoselskij Iteration

A simple potential fix for DGM stability without turning to flux updates or modifying the operator in any way is the Krasnoselskij iteration, presented in Sec. 2.2.2. For a general DGM problem, with eigenvector ψ and $\tilde{\psi} \equiv \mathbb{D}(\psi)$, this is:

$$\psi^{(n+1)} = (1-\lambda)\psi^{(n)} + \lambda\tilde{\psi}^{(n)}. \tag{39}$$

Consider again the second case of the simple example, with $\Sigma_{t,2} = 3$ cm^{-1}. Using $\lambda = 0.7$, the procedure is found to stably converge to the true solution. With a convergence criteria of 10^{-5} on eigenvalue, 39 iterations are required to reach the solution.

In the same simple example, if all cross sections are held constant aside from $\Sigma_{t,2}$, larger values of $\Sigma_{t,2}$ require smaller values of λ for stability. For example, a value of $\Sigma_{t,2} = 100$ cm^{-1} requires $\lambda \lesssim 0.02$. Although choosing a very small value of λ ensures stability for any conditions, it also greatly slows convergence. Table 1 summarizes the iterations required to reach the solution for various choices of $\Sigma_{t,2}$ and λ. This clearly shows that choosing very low values of λ can slow the convergence process greatly. It also clearly demonstrates the

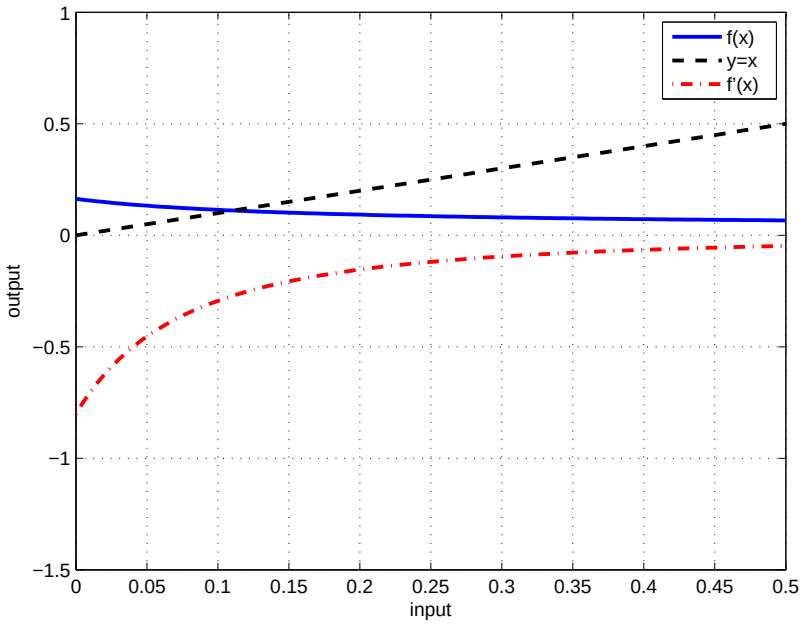

Figure 3: Input versus output thermal to fast flux ratios for DGM with flux update

concept of λ_{opt}. Although $\Sigma_{t,2} = 2$ cm^{-1} converges with Picard iteration, Krasnoselskij with $\lambda = 0.7$ reduces the required number of iterations by a factor of 4.

Consider now a larger problem, that of an infinite medium of a UO_2-water mixture with the SHEM361 group structure. Number densities are given in Tab. 2. The coarse-to-fine group map is taken to be a $361 \rightarrow 12$ group map with approximately 30 fine groups in each coarse group. Type II DCTs are used as the discrete basis set. Without flux updates, this problem is unstable with Picard iteration. However, using the Krasnoselskij iteration procedure, convergence can be achieved. The maximum stable value of λ is found to be 0.025. To achieve a convergence of 10^{-5} on eigenvalue, 1610 iterations are required. Thus, while Krasnoselskij allows for stability in the DGM recondensation procedure, the very small values of λ required for stability with an arbitrary group map on realistic data lead to very high computational expense.

4.2.1. Modified Krasnoselskij Iteration

In the 361-group infinite medium example problem, for cases in which the DGM procedure did not converge, large errors were seen to develop in groups that contain resonances. In these groups, fluxes are

Table 1: Iterations required for convergence of Krasnoselskij procedure

$\Sigma_{t,2}$ [cm^{-1}]	$\lambda = 1$	$\lambda = 0.7$	$\lambda = 0.2$	$\lambda = 0.02$
2	39	9	29	256
3	-	39	23	214
10	-	-	25	123
100	-	-	-	68

Table 2: Number densities used in SHEM361 infinite medium example problem

Isotope	Number Density [a/b−cm]
H-1 (H_2O)	0.029754258
O-16	0.034689322
U-235	0.0002575585
U-238	0.009648538

expected to be near zero. Fluxes are seen to become negative in these groups and, rather than be corrected by the iteration scheme, lead to increasingly large errors.

This observation leads to a possible modification of the Krasnoselskij iteration procedure for improved performance. Because the instabilities appear to be driven by groups with large cross sections, a smaller value of λ can be applied to the flux in those groups, whereas larger values can be applied to the non-resonant groups.

To apply this procedure, one needs to determine the number of sets to split the fine groups into that would have a unique λ value—with these sets being dubbed "levels" for the purposes of this study. Next, λ values must be selected for each level.

This procedure was applied to the SHEM361 infinite medium problem. Three cases are considered: a one-level, a two-level, and a four-level modified Krasnoselskij iteration procedure. Table 3 summarizes the values of λ used for each level in the iteration procedure. The values were chosen by trial and error, maximizing λ while maintaining stability of the procedure.

Figure 4 shows a plot of eigenvalue versus iteration for each of the three cases. These results show that applying different values of λ to each fine group does not improve estimates of the eigenvalue at early iterations. However, the modified procedure does allow the eigenvalue to converge to the reference solution in less total iterations. No choice of λ values in this procedure allowed for a converged solution to be obtained in less than the 150-250 iterations shown for the two- and four-level results.

It should be noted that the four-level procedure produces a curious convergence behavior. The eigenvalue plateaus with respect to iteration at a few points in the procedure and improves with respect to the reference very quickly between these plateaus. This demonstrates that by selecting λ in a piecewise manner as done here causes the error associated with each subset of groups to be reduced independently. Thus, during the

Table 3: λ values for modified Krasnoselskij iteration procedures

Groups	One-Level	Two-Level	Four-Level
$\Sigma_{tg} < 0.01\ \Sigma_{t,max}$	0.025	1.0	1.0
$\Sigma_{tg} \in [0.01, 0.05)\ \Sigma_{t,max}$	0.025	0.025	0.5
$\Sigma_{tg} \in [0.05, 0.20)\ \Sigma_{t,max}$	0.025	0.025	0.2
$\Sigma_{tg} > 0.20\ \Sigma_{t,max}$	0.025	0.025	0.025

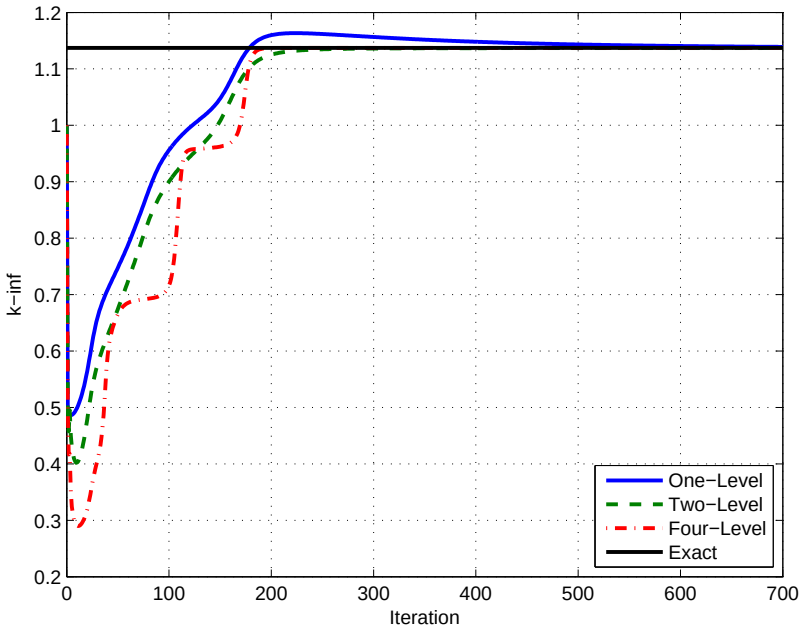

Figure 4: Eigenvalue versus iteration for modified Krasnoselskij procedure

iteration procedure, the dominant source of error in the eigenvalue shifts from one subset of groups to the next.

Because of the large number of iterations required to achieve a close approximation of the reference, the modified Krasnoselskij is not a viable solution method. Stability issues arising from large cross sections must be addressed through the choice of group map rather than through carefully chosen λ values.

A similar procedure as the one presented here could be made by applying a carefully selected value of λ in each coarse group rather than each fine group. This would require coarse groups containing resonances to use very small λ values, and so the issue of slow convergence would not be obviated. Although not studied in this work, such a procedure could provide a marginal benefit to a compatible iteration scheme.

4.3. Group Map

In the DGM method, a degree of freedom is the selection of the mapping between the fine and coarse group structures. In [10], the mapping was shown to greatly influence the convergence rate of the recondensation procedure. The observed behavior did not show a simple relationship between the number of coarse groups and the convergence rate. However, because of the use of flux updates in this study, the impact of the group map on stability was not considered.

The selection of the group map is of great importance to the stability characteristics of the method. As seen in the preceding simple 2 group example, relatively small disparities in cross sections can lead to instability. Ideally, a procedure to improve the stability—*i.e.* enabling large λ values to be used with Krasnoselskij iteration and reducing the problem dependent nature of the choice of λ—is desired. A well-chosen group

map is one way to accomplish this.

To understand the effect of the group map on the stability of the method, consider now a 10 group infinite medium problem as an illustrative example.

In this example, the total cross section is taken to have a large cross section in groups 5-7—analogous to a resonance—and a much smaller but noisy cross section in the other groups, as shown in Fig. 5. The fission and scattering sources were taken to be as simple as possible so as not to influence the results.

Figure 6 shows two potential group maps with three coarse groups. The first is an arbitrarily selected map, which includes an enormous range of magnitudes of cross sections in the second coarse group. The second map still uses three coarse groups, but shifts the boundaries such that the resonance analog is fully contained within the second coarse group.

In both cases, Krasnoselskij iteration can be used to stably converge to the known solution. In the first mapping, the maximum stable choice of the λ parameter was found by trial and error to be 0.23. The fastest converging choice was found to be 0.22, leading to convergence of 10^{-5} on the eigenvalue in 64 iterations. In the second mapping, λ values as high as 0.9 are seen to lead to convergence, and a choice of 0.7 leads to convergence in only 17 iterations. This clearly shows a strong relationship between the mapping and the efficiency of the algorithm.

Although this simple illustrative example demonstrates the necessity of a strong choice of a group map, it does not fully define an algorithm to do so. However, these ideas can easily be applied to more substantial problems to create such an algorithm.

With this in mind, possible group maps were investigated. It was found that disparities in cross sections inside coarse groups more strongly affect stability via their ratio than a simple difference. Thus, a group mapping algorithm should seek to limit the ratio of the minimum to maximum total cross section inside a coarse group.

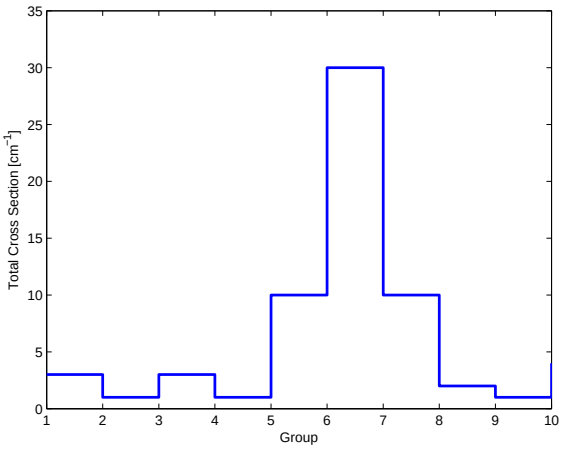

Figure 5: Total cross section for 10 group example problem

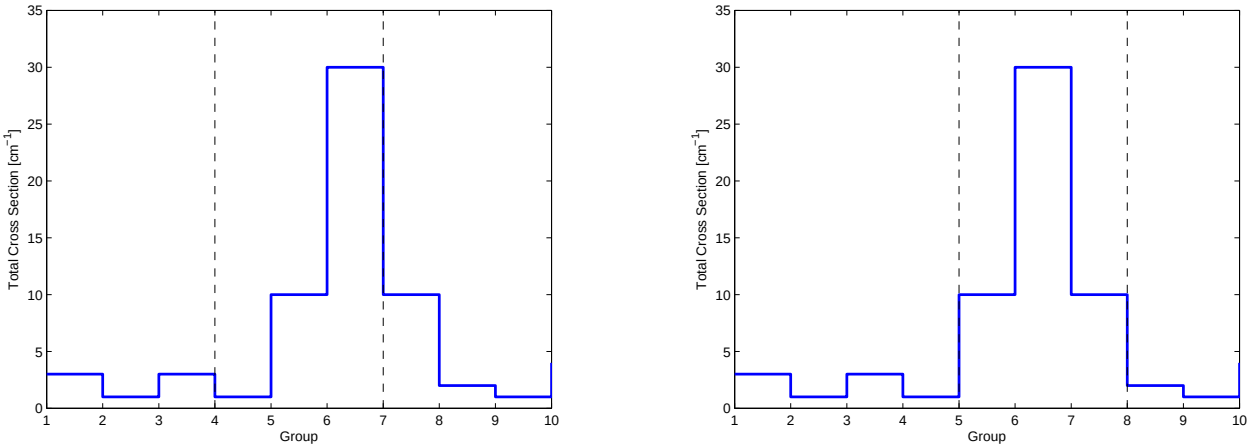

Figure 6: Poor choice of group map (left); Good choice of group map (right)

It was found that regions with small cross sections do not greatly affect the stability of the solution scheme, even if the ratio of cross sections becomes large. This is a fairly intuitive result, as regions with small reaction rates are unlikely to greatly influence the overall solution. Thus, a group mapping algorithm should not apply the limit on the ratio below a threshold cross section.

In [10], the maximum number of fine groups per coarse group without compromising stability was sought. Using Discrete Legendre Orthogonal Polynomials, a loss of orthogonality is observed when they are generated with either a recursion relation or directly with a Rodrigues formula. However, with Discrete Cosine Transforms, a loss of orthogonality is not seen, as arbitrary order basis sets can be generated with simple cosine evaluations. However, there is still an optimal number of fine groups per coarse group, as increased computational expense of moment generation will eventually outweigh the savings from the reduction in groups in the eigenproblem. Thus, regardless of the basis, a group mapping algorithm should limit the number of fine groups per coarse group.

Finally, it is recognized that certain group boundaries are convenient for reasons other than stability. For instance, if one desires to generate two-group reaction rates, it is preferred to force a coarse group break at a given two-group boundary. In past work [4], it was also observed that forcing a group break at the top upscatter group is beneficial computationally for most thermal reactor problems. Forcing group breaks has not been observed to adversely affect stability, and so this can be included in any group mapping algorithm.

This leaves us with the following basic algorithm to choose a group map:

Basic algorithm:

1. Limit ratio of smallest to largest cross section in coarse group.
2. Relax ratio condition for coarse groups with only small cross sections.
3. Cap number of fine groups per coarse group.

4. Force coarse group breaks where desired.

Recommended limits are:

- Smallest to largest cross section ratio: 2
- Small cross section limit: 1.5 cm^{-1}
- Maximum fine groups per coarse group: 60.

These limits are likely not optimal, but have been found to lead to stable DGM solutions for all problems considered with Krasnoselskij iteration with $\lambda \leq 0.7$. Both the ratio and small cross section limits were attempted to be maximized while still assuring stability. The maximum number of fine groups per coarse group was less rigorously selected as an attempt to balance moment generation expense with savings from the smaller eigenproblem.

It should be noted that these limits and the optimal λ are certainly problem dependent, but the key is to find a simple algorithm that provides most of the desired effect. The problem dependent nature of the relaxation parameter λ is expected, as it is encountered in other relaxation schemes, including linear solvers and multi-physics calculations. In general, a set of limits that works for all problems is undoubtedly overly conservative for certain problems. Also, the limits could be adjusted to allow other values of λ to be stable, including Picard iteration; however, there is little motivation for this at this time. The balance required for determining the maximum fine groups per coarse group is a function of many variables including the number of unknowns, the dominance ratio, *etc.*

Now, the example problem of an infinite medium comprised of a UO_2-water mixture with the SHEM361 group structure is revisited with this group mapping algorithm. Consider the two group maps, shown in Fig. 7 and Fig. 8.

The first arbitrarily sets 9 fine groups per coarse group, resulting in 40 coarse groups. In order for convergence to be achieved, Krasnoselskij iteration is needed with a maximum λ of 0.032. As expected with such a small value of λ, convergence is extremely slow, requiring 404 iterations.

The second map uses the proposed group map algorithm with recommended limits. This also leads to a coarse group structure of 40 coarse groups. In this map, group boundaries are concentrated near the major resonances. In non-resonant fine groups, much larger coarse groups are observed. Krasnoselskij iteration is convergent for all values of λ, including the case of Picard iteration or $\lambda = 1$. Only 49 iterations are required for the same level of convergence.

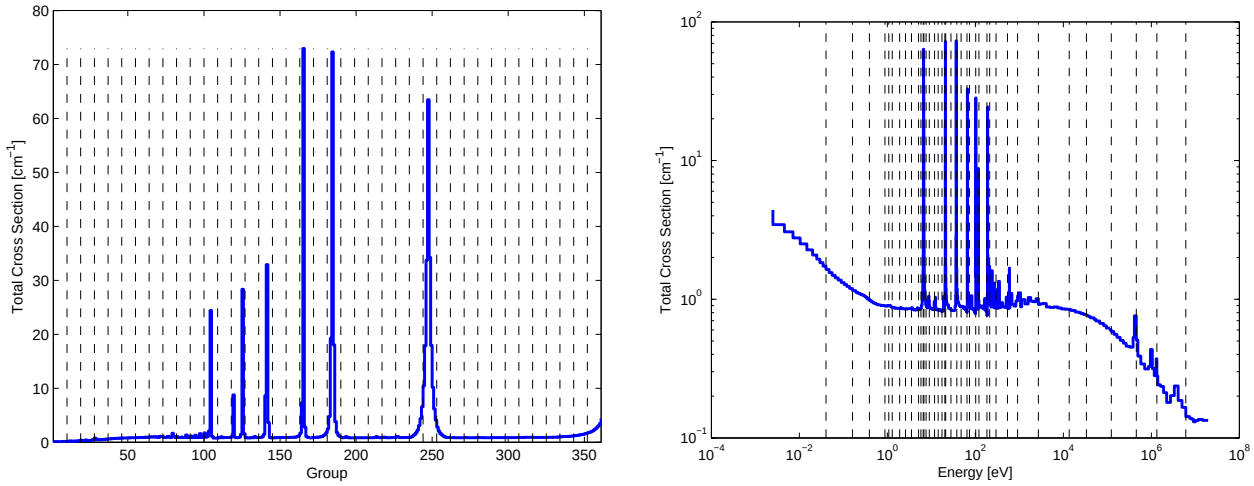

Figure 7: Poor choice of group map, 9 fine groups per coarse group

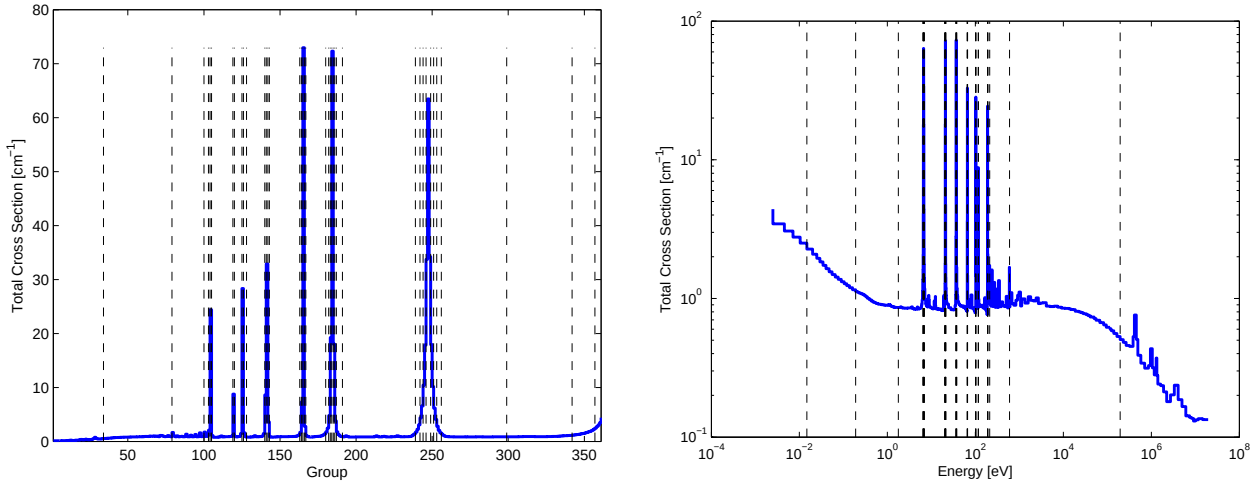

Figure 8: Good choice of group map, coarse group boundaries at jumps in cross section

It is clear that an informed choice of group map is a necessity for the DGM method without flux updates. As cases with more groups are considered, it is expected that the ratio of fine groups to coarse groups will decrease. With more groups, resonances are better resolved, leading to lesser disparity in neighboring groups. Furthermore, in non-resonant energy regimes, many more coarse groups with large numbers of fine groups can be expected.

5. BWR Core Benchmark

5.1. Problem Description

A 1-D computational benchmark problem is used to demonstrate the methods developed in this paper. The benchmark is adapted from the benchmark problem presented in [8]. BWR reactors are modeled in slab geometry with a series of seven assemblies. Each assembly is made up of two half slabs of water surrounding four fuel slabs. These cores represent both supercritical and subcritical systems, varying amounts of highly absorbing materials present (as gadolinium mixed in with the fuel), and different fissile materials. The geometry is shown in Fig. 9.

Each fuel slab is 3.2512 cm in width; each water half slab is 1.1176 cm in width. Thus, each assembly is 15.24 cm and the full core is 106.68 cm in width. Core 1 is taken from reference [8], where it was labeled Core 2. It features a small amount of gadolinium in alternating assemblies. Core 2, introduced for this study, alternates between UO_2 and MOX fueled assemblies. Fuel 1 is a low enriched fuel, with approximately 2% U-235. Fuel 2 is a higher enrichment, with approximately 4% U-235. The MOX fuel is approximately 90% uranium with the higher enrichment and 10% minor actinides. Table 4 gives the isotopic compositions of each of the materials in the benchmark problem.

Solutions are obtained using the discrete ordinates method. A 10-point Gauss-Legendre quadrature is used. Only isotropic scattering is considered. To ensure clarity in the results by maintaining full consistency and isolating the enegy component, the step difference spatial discretization is used. The S_{10} solver, used both for a reference and in the DGM equations, is unaccelerated. A uniform mesh spacing of 0.4 cm is used. Two energy group structures are considered, SHEM361 and NG2042. All calculations were performed in a Fortran 2003 implemenation and run on a desktop computer with an Intel i7-870 CPU @ 2.93 GHz. DGM solutions are performed both with Krasnoselskij iteration with varying choices of λ and with the flux update method with varying numbers of flux updates. Type II DCTs are used as the discrete basis set. The group mapping algorithm is used with the recommended limits from Sec. 4.3. Reference solutions are taken to be direct fine group solutions. In all cases, starting guesses for the fluxes are constant group fluxes in all fine groups and spatial meshes.

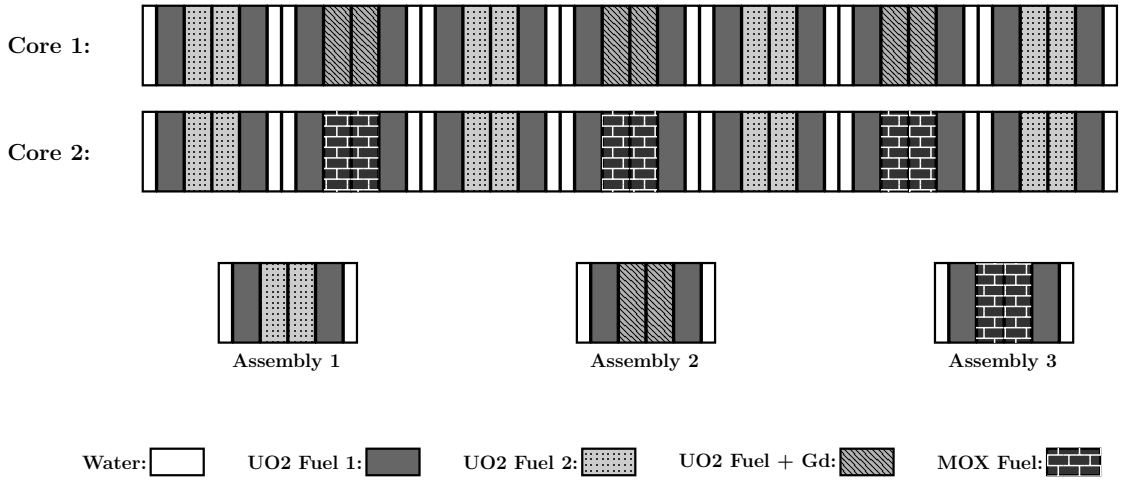

Figure 9: Geometry of 1-D BWR benchmark problem

Table 4: Isotopic compositions of materials in 1-D BWR benchmark problem

Isotope	Concentration [$^{a}/_{b \cdot cm}$]				
	Water	UO_2 Fuel 1	UO_2 Fuel 2	UO_2 Fuel 2 + Gd	MOX Fuel
H-1	4.03E-2	2.73E-2	2.73E-2	2.73E-2	2.73E-2
O-16	2.02E-2	2.87E-2	2.87E-2	2.86E-2	2.86E-2
Zr-0	7.86E-3	4.79E-3	4.79E-3	4.79E-3	4.79E-3
U-234	-	1.50E-6	2.52E-6	2.63E-6	2.32E-6
U-235	-	1.68E-4	2.75E-4	2.87E-4	2.53E-4
U-238	-	7.39E-3	7.28E-3	6.88E-3	6.70E-3
Gd-154	-	-	-	9.68E-6	-
Gd-155	-	-	-	6.58E-5	-
Gd-156	-	-	-	9.10E-5	-
Gd-157	-	-	-	6.96E-5	-
Gd-158	-	-	-	1.10E-4	-
Gd-160	-	-	-	9.80E-5	-
Np-237	-	-	-	-	3.23E-5
Pu-238	-	-	-	-	1.59E-5
Pu-239	-	-	-	-	2.93E-4
Pu-240	-	-	-	-	1.32E-4
Pu-241	-	-	-	-	6.38E-5
Pu-242	-	-	-	-	3.76E-5
Am-241	-	-	-	-	2.04E-5
Am-242	-	-	-	-	1.05E-5

5.2. Results

5.2.1. Exploration of the Relaxation Parameter Space

Cores 1 and 2 were solved with several values of λ. Table 5 gives the summary of group maps used for these problems. Figure 10 and Fig. 11 show results with the SHEM361 group structure for Cores 1 and 2, respectively. Figure 12 and Fig. 13 show results with the NG2042 group structure for Cores 1 and 2, respectively.

In all cases, the optimal value of λ was found to correspond to the maximum stable value. For both cores with the SHEM361 group structure, the maximum stable value of λ is approximately 0.8. With the NG2042 group structure, clear instabilities are not seen, but the convergence behavior is not as smooth as desired with $\lambda = 1$. Thus, the maximum stable value of λ can be considered to be approximately 0.9.

Note, though, that the instabilities set in after the initial improvement in reaction rates from the first few iterations. The value of λ could be reduced after the first few iterations to gain the faster early convergence but avoid the instabilities. This would be a shift from Krasnoselskij iteration to Mann iteration. However, the λ trajectory must be determined *a priori* if there is to be any benefit. Any algorithm to observe the oscillatory behavior characteristic of instability and adjust λ accordingly would be outperformed by an initially stable choice of λ.

The optimal choice of λ is certainly a problem dependent quantity. However, these results demonstrate that the sensitivy to the choice of λ is not very significant. Thus, rather than seeking to use a truly optimal value, a value that is found to work for most cases can be used to simplify problem setup.

Also in all cases, the convergence behavior is seen to exhibit a shoulder. That is, reaction rate errors decrease quickly for the first several iterations, but ultimately reach a slower asymptotic convergence rate. Because the desired use of the recondensation procedure is to improve reaction rates with only a few recondensation steps, slow asymptotic convergence is not a concern.

Note that the number of iterations to achieve convergence decreases significantly when moving from the SHEM361 group structure to the NG2042 group structure. This can be explained by considering the fine group structures. The SHEM361 group structure contains very disparate cross sections in neighboring groups, as it represents the resonance structure with very few groups. Thus, the solution is very dependent upon the fine group detail, and the map to a coarse group structure struggles to pick up the spectral effects. For the NG2042 group structure, resonances are represented with many more groups, leading to smoother cross sections. Thus, the influence of the higher order solutions is reduced, and the coarse group solution better

Table 5: Fine-to-coarse group maps for BWR benchmark calculations

Structure	Core 1	Core 2
SHEM361	$361 \rightarrow 40$	$361 \rightarrow 46$
NG2042	$2042 \rightarrow 86$	$2042 \rightarrow 89$

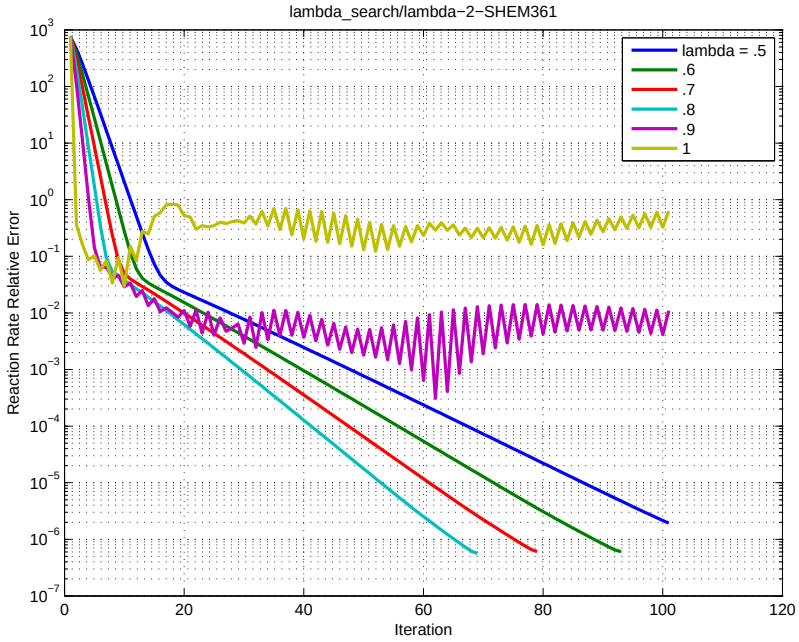

Figure 10: Core 1 reaction rate errors, SHEM361 group structure

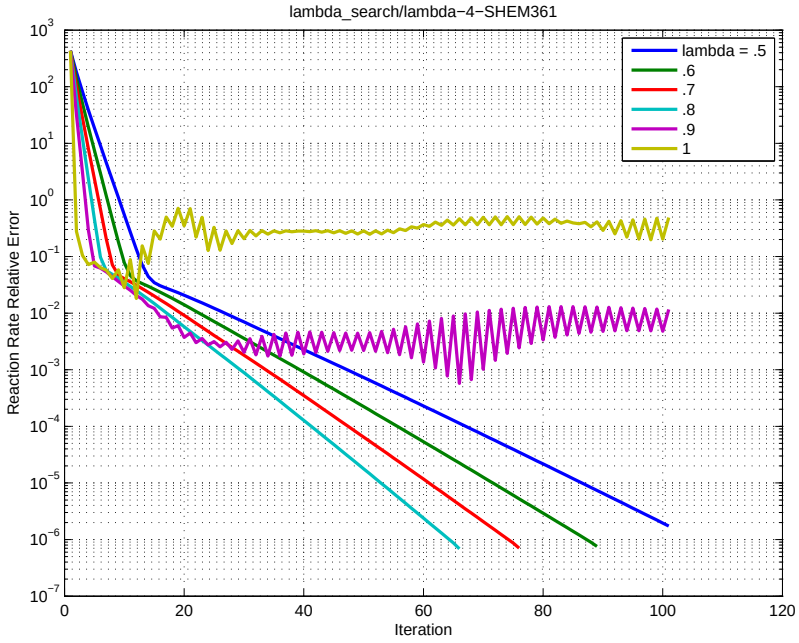

Figure 11: Core 2 reaction rate errors, SHEM361 group structure

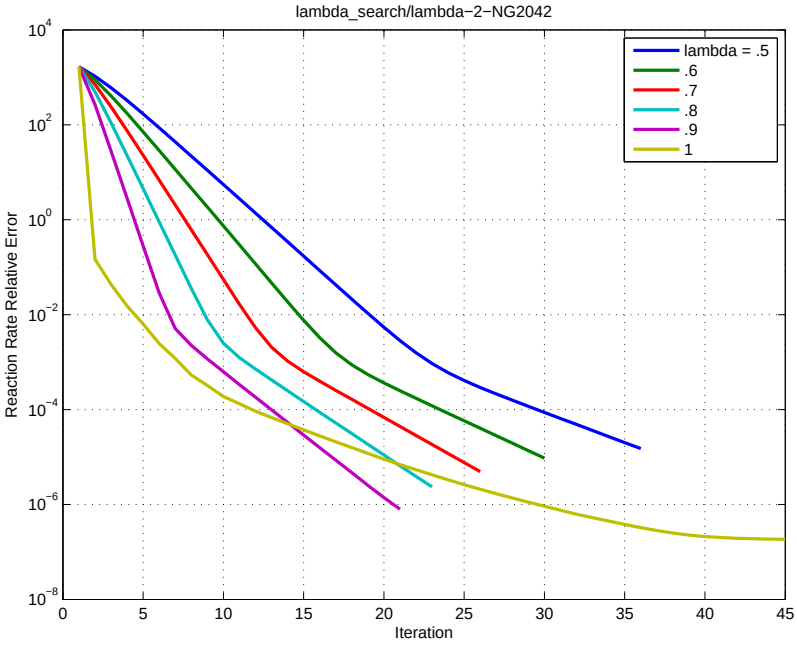

Figure 12: Core 1 reaction rate errors, NG2042 group structure

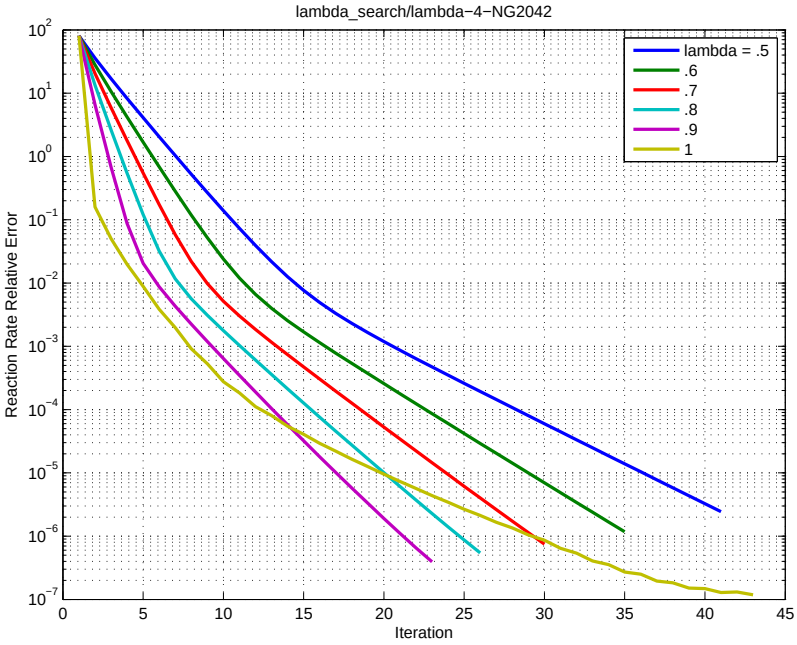

Figure 13: Core 2 reaction rate errors, NG2042 group structure

represents the true solution. Results are expected to improve even further as ultra-fine libraries are used.

5.2.2. Comparison of Power Iteration, DGM with Krasnoselskij Iteration, and DGM with Flux Updates

Convergence behavior and timing results for Cores 1 and 2 are compared to power iteration. DGM calculations used Krasnoselskij iteration with the maximum stable λ as determined previously and also with a lesser value of λ. Convergence for these comparisons is defined on the fine group fluxes as:

$$\left[\frac{1}{N_g N_{\Delta x}} \sum_g \sum_i \left(\phi_g^{(n)}(x_i) - \phi_g^{(n-1)}(x_i)\right)^2\right]^{1/2} < 10^{-8}, \tag{40}$$

where N_g is the number of fine groups, $N_{\Delta x}$ is the number of spatial meshes, and $\phi_g^{(n)}(x_i)$ is the flux in fine group g at mesh point x_i at iteration n. This is a normalized L_2 norm for the group fluxes.

Table 6 shows the group maps used for these comparisons. With the group mapping algorithm (notated as GMA), the same structures as the previous section are used. Without the group mapping algorithm, an equal number of fine groups per coarse group is used for all but the last group. With SHEM361, 30 fine groups per coarse group is used; for NG2042, 50 fine groups per coarse group is used.

Table 7 gives timing and iteration comparisons for the SHEM361 group structure. Table 8 gives the same table for the NG2042 group structure. In these tables, the power iteration row gives results for direct power iteration, not using DGM. The remaining rows give DGM results, starting with Krasnoselskij iteration and the proposed group mapping algorithm in lieu of flux updates and continuing to varying numbers of flux updates with and without the group mapping algorithm.

Note that iteration counts compared between direct power iteration and the DGM methods in this context are not equivalent. A DGM iteration represents a full recondensation step, including a fully converged spatial solution on the coarse group. The power iterations are single fine group fixed source solutions, connected by the standard power iteration procedure.

For the SHEM361 structure, direct power iteration does quite well in comparison to DGM. Krasnoselskij iteration requires quite a large number of iterations for convergence, and so performs poorly in terms of overall time. With flux updates, computational time is reduced as additional flux updates are performed. Using the group mapping algorithm, only a single flux update is needed for stability. Without the group

Table 6: Group maps used for comparison cases

Structure	Method	Core 1	Core 2
SHEM361	GMA	$361 \rightarrow 40$	$361 \rightarrow 46$
SHEM361	No GMA	$361 \rightarrow 12$	$361 \rightarrow 12$
NG2042	GMA	$2042 \rightarrow 86$	$2042 \rightarrow 89$
NG2042	NO GMA	$2042 \rightarrow 41$	$2042 \rightarrow 41$

Table 7: Timing results for benchmark problem with SHEM361 group structure

Method	Core 1		Core 2	
	Iterations	Time [s]	Iterations	Time [s]
Power Iteration	206	69.6	175	53.1
Krasnoselskij, $\lambda = 0.7$, GMA	51	600.2	50	490.7
Krasnoselskij, $\lambda = 0.8$, GMA	45	531.9	44	435.8
1 Flux Update, GMA	15	174.9	14	147.1
3 Flux Updates, GMA	11	128.8	11	109.0
5 Flux Updates, GMA	10	120.9	10	97.3
12 Flux Updates, GMA	6	87.1	6	71.3
1 Flux Update, No GMA	-	-	-	-
3 Flux Updates, No GMA	-	-	-	-
5 Flux Updates, No GMA	-	-	-	-
12 Flux Updates, No GMA	6	42.1	6	39.3

Table 8: Timing results for benchmark problem with NG2042 group structure

Method	Core 1		Core 2	
	Iterations	Time [s]	Iterations	Time [s]
Power Iteration	116	2796.6	92	1730.7
Krasnoselskij, $\lambda = 0.8$, GMA	11	1207.0	12	1188.7
Krasnoselskij, $\lambda = 0.9$, GMA	10	1061.6	11	1102.2
1 Flux Update, GMA	6	699.8	6	661.0
3 Flux Updates, GMA	4	568.5	4	543.7
5 Flux Updates, GMA	4	658.2	4	623.2
12 Flux Updates, GMA	3	718.3	4	918.6
1 Flux Update, No GMA	-	-	-	-
3 Flux Updates, No GMA	-	-	-	-
5 Flux Updates, No GMA	5	770.8	5	751.1
12 Flux Updates, No GMA	4	920.4	4	907.7

mapping algorithm, 12 flux updates are needed to ensure stability of Core 1; 10 updates are needed for Core 2.

Note that in this case, the DGM solution can be accelerated by performing a single power iteration before beginning the DGM procedure. This allows the computational time associated with the DGM solution to be approximately the same as the power iteration results. By alternating between power iterations and DGM recondensation steps, full convergence can be accelerated. This observation was not studied in detail, as accelerating the fine group solution is not the goal of this study. However, this suggests that DGM can be used to accelerate power iteration in some cases. Similar work was previously performed in [9].

For the NG2042 structure, DGM outperforms power iteration in all stable cases considered. Krasnoselskij iteration requires approximately double the number of iterations as the flux update cases. Although it still is outperformed by the flux update method, the discrepancy is greatly reduced from the SHEM361 case. With the group mapping algorithm, adding additional flux updates does not necessarily provide a

computational benefit, as the number of iterations does not decrease at the same rate. Without the group mapping algorithm, 5 flux updates are needed for stability; a single flux update still yields stability with the group mapping algorithm.

Note that some of the discrepancy in times between power iteration and DGM in the NG2042 case can be attributed to growing issues with memory management. As the problem size grows, much of the performance is driven by cache efficiency. Because DGM shrinks the size of the transport problem, it allows the transport solution to be more cache efficient, even in naive implementations. Note that performance-oriented power iteration implementations, such as in the DETRAN discrete ordinates code [18], can reduce the computational cost of power iteration to that of the unaccelerated DGM solution.

Comparable to the problem dependent nature of the optimal choice of λ with Krasnoselskij iteration, the number of flux updates required for stability with the flux update method is also problem dependent. However, the group mapping algorithm greatly improves the stability and allows many fewer flux updates to be necessary. The issue of the optimal number of flux updates for minimum computational time remains problem dependent, though.

The breakdown of time spent during the DGM calculations shifts from coarse group transport and higher order solutions with the SHEM361 structure to moment generation with the NG2042 structure. Tables 9 and 10 show the breakdown for a few of the cases considered. The column labeled "CG TE + HO" represents the time spent solving the coarse group transport equation and the higher order equations.

Table 9: Breakdown of time spent in DGM solutions of Core 1 using the SHEM361 library

	Computational Time [s]		
Method	Moment Generation	CG TE + HO	Flux Updates
Krasnoselskij, $\lambda = 0.8$, GMA	125.2	471.6	-
1 Flux Update, GMA	36.6	135.8	2.3
12 Flux Updates, GMA	14.6	61.4	11.0
12 Flux Upates, No GMA	11.5	19.4	11.2

Table 10: Breakdown of time spent in DGM solutions of Core 1 using the NG2042 library

	Computational Time [s]		
Method	Moment Generation	CG TE + HO	Flux Updates
Krasnoselskij, $\lambda = 0.9$, GMA	904.9	293.2	-
1 Flux Update, GMA	499.8	134.9	64.7
5 Flux Updates, GMA	336.0	105.4	216.5
5 Flux Upates, No GMA	427.7	70.5	272.4

6. Conclusions and Future Work

Through consideration of the stability of the Discrete Generalized Multigroup method, two algorithmic changes were proposed to the recondensation procedure. First, the iteration procedure can be relaxed with Krasnoselskij iteration, which allows convergence without flux updates. Second, a group mapping algorithm was developed to improve stability by avoiding large fluctuations in fine group cross section values within a coarse group.

Although the Krasnoselskij iteration scheme was not shown to be a benefit directly in terms of computational expense, it still provides new options for the DGM method. Because it obviates the need for fine group sweeps, Krasnoselskij iteration allows the collision and transport terms in the transport equation to have a different number of energy groups than the source terms, so long as an equivalent coarse group structure is used. Also, it greatly reduces the computational cost per DGM iteration, which could be a benefit in calculations where full convergence is not desired; rather, fast improvement over the initial coarse group solution could be desired.

The group mapping algorithm was shown to greatly improve stability, allowing values of λ much closer to unity with Krasnoselskij iteration or many fewer flux updates with the standard recondensation procedure. For future work, the group mapping algorithm presented here could potentially be improved by considering reaction rates rather than total cross sections to determine group boundaries. In this case, the group map would change from iteration to iteration, adding some slight complication to the iteration process and measures of convergence.

With large numbers of groups, the bulk of the computational expense with DGM is in the computation of scattering moments. However, the nature of DGM allows novel approaches to approximating the scattering kernel. As future work, the coarse group scattering kernel and moments could be generated on the fly inexpensively. Alternatively, the aformentioned scattering matrix with a different energy mesh than the collision terms is also feasible to implement.

Acknowledgments

This research was performed under appointment of the first author to the Rickover Fellowship Program in Nuclear Engineering sponsored by Naval Reactors Division of the U.S. Department of Energy.

References

References

[1] Robert E. Macfarlane. *PSR-480/NJOY99.0: Code System for Producing Pointwise and Multigroup Neutron and Photon Cross Sections from ENDF/B Data.* Los Alamos National Laboratory, 2000.

[2] Nicholas Horelik, Bryan Herman, Benoit Forget, and Kord Smith. Benchmark for evaluation and validation of reactor simulations (BEAVRS). *International Conference on Mathematics and Computational Methods Applied to Nuclear Science & Engineering*, 2013.

[3] Brian N. Aviles, Daniel J. Kelly, and Bryan R. Herman. MC21 analysis of the MIT PWR benchmark: Hot zero power results. *International Conference on Mathematics and Computational Methods Applied to Nuclear Science & Engineering*, 2013.

[4] Lei Zhu and Benoit Forget. An energy recondensation method using the discrete generalized multigroup energy expansion theory. *Annals of Nuclear Energy*, 38:1718–1727, 2011.

[5] Steven Douglass and Farzad Rahnema. Consistent generalized energy condensation theory. *Annals of Nuclear Energy*, 40:200–214, 2012.

[6] Mark L. Williams and Kang-Seog Kim. The embedded self-shielding method. *PHYSOR 2012 – Advances in Reactor Physics Linking Research, Industry, and Education*, 2012.

[7] Lei Zhu and Benoit Forget. A discrete generalized multigroup energy expansion theory. *Nuclear Science and Engineering*, 166:239–253, 2010.

[8] Farzad Rahnema, Steven Douglass, and Benoit Forget. Generalized energy condensation theory. *Nuclear Science and Engineering*, 160:41–58, 2008.

[9] Lei Zhu and Benoit Forget. A nonlinear acceleration method. *Transactions of the American Nuclear Society*, June 2011.

[10] Nathan A. Gibson and Benoit Forget. Application of the discrete generalized multigroup method to ultra-fine energy mesh in infinite medium calculations. *PHYSOR 2012 – Advances in Reactor Physics Linking Research, Industry, and Education*, 2012.

[11] Lei Zhu. *Discrete Generalized Multigroup Theory and Applications*. PhD thesis, Massachusetts Institute of Technology, 2012.

[12] Nathan A. Gibson and Benoit Forget. Eliminating flux updates from the discrete generalized multigroup method. *Transactions of the American Nuclear Society*, November 2012.

[13] Vasile Berinde. *Iterative Approximation of Fixed Points*, volume 1912 of *Lecture Notes in Mathematics*. Springer, second edition, 2004.

[14] M. A. Krasnoselskij. Two remarks on the method of successive approximations. *Uspehi Mat. Nauk.*, 10(1/63):123–127, 1955. (Russian).

[15] N. Hfaiedh and A. Santamarina. Determination of the optimized SHEM mesh for neutron transport calculations. *Mathematics and Computation, Supercomputing, Reactor Physics and Nuclear and Biological Applications*, 2005.

[16] A. Hébert and A. Santamarina. Refinement of the Santamarina-Hfaiedh energy mesh between 22.5 eV and 11.4 keV. *International Conference on Reactor Physics, Nuclear Power: A Sustainable Resource*, 2008.

[17] Alain Aggery. Calculs de reference avec un maillage multigroupe fin sur des assemblages critiques par APOLLO 2. Technical Report CEA-N-2848, Commissariat à l'Energie Atomique – France, Décembre 1999. (French).

[18] Jeremy A. Roberts. *libdetran: Deterministic Transport Utilities*. Massachusetts Institute of Technology, 2012. `http://github.com/robertsj/libdetran`.